Numerical Simulation of Dust Cake Build-up and Detachment on Rigid Ceramic Filters for High Temperature Gas Cleaning

[1]T.G. Chuah, [2]J.P.K.Seville

[1]Department of Chemical and Environmental Engineering, Faculty of Engineering, Universiti Putra Malaysia, 43400 UPM Serdang, Selangor.

[2]Department of Chemical Formulation Engineering, School of Engineering, University of Birmingham, Edgbaston, B15 2TT Birmingham, United Kingdom.

ABSTRACT

Rigid ceramic filters have proved themselves as highly efficient gas filtration devices. However, the filter cleaning mechanisms by which deposited cake is removed from the filter surface are still not fully understood. A mathematical model that is capable of simulating the time-dependent build-up of dust filter cakes, on the surface of filter, including the calculation of the corresponding pressure drop and the thickness of filter cake which formed during the filtration is proposed. The model also simulates the regeneration of the filter medium and predicts the residual pressure drop after regeneration. This paper focuses on the first basic mechanism of regeneration, the forming and the detachment of the dust filter cake. This enables the simulation of several cycles of filtration and regeneration to investigate the long-term-behaviour of a dust filter.

Keywords : *Rigid ceramic filters, dust cakes, filtration cycles, residual pressure drop, incompressibility*

INTRODUCTION

Periodically regenerable cake-forming filters are used to separate particles from gases with high dust concentrations, whereby the separation arises as the dust-gas mixture passes through the filter medium and the particles are retained. During the build-up of the filter cake the pressure drop over the filter increases, making a regeneration of the filter medium indispensable. The regeneration is performed at a defined maximum pressure drop across the filter and after regeneration the next filtration-cycle starts and a new dust filter cake is built-up on the cleaned filter medium.

The residual pressure drop is a measure of the dust remaining in the depth of the filter medium. Unfortunately, it quite often happens that the residual pressure drop does not reach a constant value after several filtration cycles, but increases steadily due to the fact that not all the filter cake is removed by cleaning. This so-called `patchy cleaning' [1, 2] affects both the residual pressure drop and the rate of pressure increase in the following filtration cycle that may lead to a breakdown of a stable operation.

The objective of this paper is to develop a mathematical model that is capable of simulating the long term build-up of dust filter cakes, on the surface of filter, including the calculation of the corresponding pressure drop along the axis of the filter during filtration. The model should also simulate of the regeneration of the filter medium and predict the residual pressure drop after regeneration. As a first step the authors concentrated on the first basic mechanism of regeneration, the forming of the dust filter cake. This enables the simulation of several cycles of filtration and regeneration to investigate the long-term-behaviour of a dust filter.

The model should also clarify the mechanism which causes the steady increase of the residual pressure drop of a dust filter over time. It was found in some previous studies that the long-term-behaviour of the residual pressure drop depended on the compressibility of the dust cake on the filter medium. Therefore, the adhesion force and the effective distance of separation between the particles were also studied.

SIMULATION OF DUST CAKE BUILD-UP ON THE FILTER MEDIUM

This section describes a physical model for cake and pressure build-up on candle filters. The model was aimed at investigating filtration operation and reverse pulse cleaning of the filter. It is useful to calculate the filter cake thickness and pressure drop along the filter candle. Figure 1 shows the schematic diagram of filter cake build-up on the filter surface.

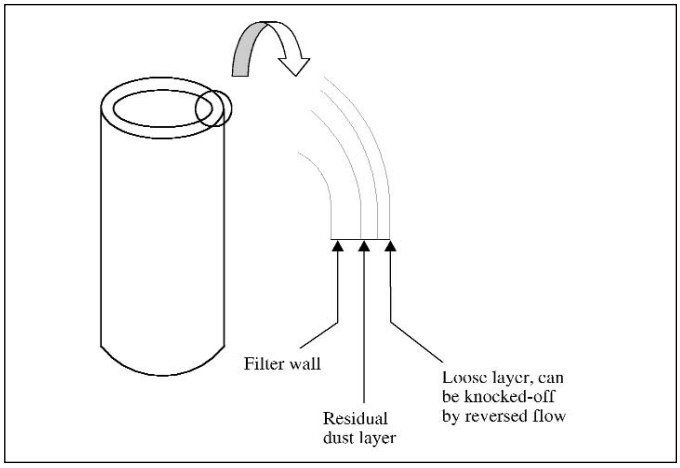

Figure 1: Schematic diagram of filter cake build-up on the filter surface

Assumptions

The model used here has to omit several factors that may affect the filtration operation and is considerably "idealised". However, this model is targeted to describe the most important physics of filtration before its secondary effects are taken into consideration.

The model derivation makes the following assumptions:

i) All particles entering the filter housing are deposited on the surface of the filter.
ii) The filter cake and the filter medium obey Darcy's law.
iii) The gas is incompressible.
iv) To simplify the model, the small area at the bottom of the filter (closed end, about 1% of the total filter surface), for which the gas flow rate differs significantly from the rest of the filter, is ignored in the subsequent analysis.

Filter 'conditioning' or 'blinding', the penetration of fine particles into the filter pores may sometimes occur and increase the pressure drop across the filter. The effect of penetration of finer particles deeper into the filter cake has recently been modelled [3]. However, it is not considered in this analysis.

Flow Through Thick Filter

[4] suggested a numerical expression to define the pressure drop through a thick-walled rigid filter. Consider a flow at face velocity, U_o, through a thick-walled cylindrical filter of outside diameter, D_o and internal diameter, D_i. The volumetric gas inflow per unit length of the filter candle is $\pi\ D_o\ U_o$. Neglecting any changes in gas density as it passes through the porous medium, the superficial velocity at any intermediate radius r is

$$U = U_o D_o / 2r \tag{1}$$

Assuming the radial flow is a viscous flow (i.e. Re is small), then Darcy's law can be applied here:

$$\frac{dP}{dr} = -k_1 \mu U = -\frac{k_1 \mu U_o D_o}{2r} \tag{2}$$

Therefore, the total pressure drop across the filter candle wall is given by:

$$\Delta P_f = \int_{\frac{D_i}{2}}^{\frac{D_o}{2}} \frac{k_1 \mu U_1 D_o}{2r}\, dr \tag{3a}$$

$$= \frac{k_1 \mu U_0 D_0}{2} \int_{\frac{D_i}{2}}^{\frac{D_o}{2}} \frac{dr}{r}$$

$$= \frac{k_1 \mu U_0 D_0}{2} \ln\left[\frac{D_o}{D_i}\right] \tag{3b}$$

Figure 2 shows a schematic diagram of flow through a thick filter candle wall. The calculation will be extended into the filter cake build-up model and will be discussed in next section.

Because of the cylindrical geometry of the filter and filter cakes, Darcy's law needs to be solved in polar coordinates. Neglecting any changes in gas density as it passes through the porous dust medium, the superficial velocity at any intermediate radius r_c as before is given by;

$$U_c = U_o \frac{D_o}{2r_c} = U_o \frac{D_o}{D_c} \tag{4}$$

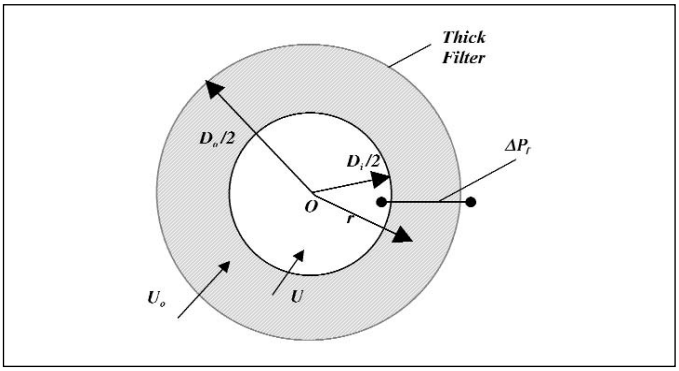

Figure 2: Schematic diagram of flow through thick filter candle.

Hence, the pressure drop across the filter cake between the filter medium and dust cake is:

$$\Delta P_c = \frac{k_2 U_c D_c}{2} ln\left[\frac{D_c}{D_o}\right] \tag{5}$$

where, k_2 is the cake resistance, D_c is the outer diameter of filter cake and U_c is the superficial velocity through the outer radius of cake (Figure 3).

The constant gas flow rate into the filter vessel, Q (volumetric flow rate per unit length), can be written as:

$$Q = \pi D_c U_c = \pi D_o U_o = \pi D_i U_i \tag{6}$$

Then, U_c can be rewritten as:

$$U_c = \left(\frac{D_o}{D_c}\right) U_o \tag{7}$$

The thickening rate of the cake formed on the surface of the filter can be determined by a dust volume balance:

$$\frac{dx}{dt} = \frac{wU_c}{\rho_c} \tag{8}$$

$$\Delta x = \int \frac{wU_c(t)}{\rho_c}\, dt \tag{9}$$

where w is the dust concentration (kg/m^3) in the gas flow, which has been taken to be constant, ρ_c is the cake density and Δt is the time interval from t=0 to time t. Cake density is defined as:

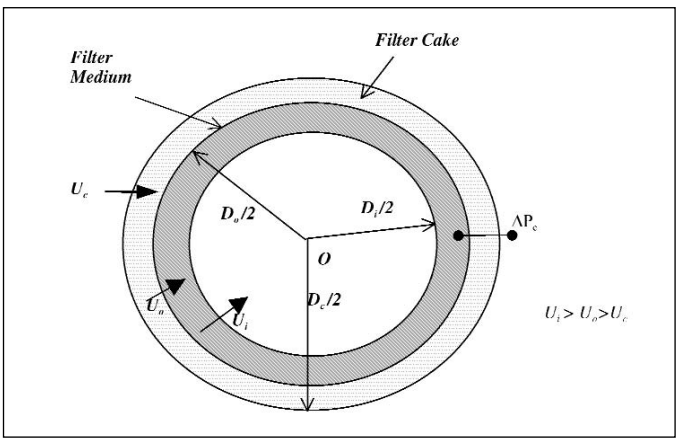

Figure 3: Schematic diagram of flow through a filter candle and filter cake.

$$\rho_c = \rho_p (1-\varepsilon_c) \quad (10)$$

where ρ_p is the particle density and ε_c is filter cake porosity. The outer diameter of the filter cake over Δt is then calculated as:

$$D_c(t) = D_o + \Delta x \quad (11)$$

The total pressure drop across the filter medium and dust cake is:

$$\Delta P_T = \Delta P_f + \Delta P_c \quad (12)$$

When $t = 0$, no cake is formed, the pressure difference is equal to the pressure difference across the clean filter.

$$\Delta P_T = \Delta P_f \quad (13)$$

When $t = t_1$, dust starts to accumulate on the filter surface, then

$$\Delta x_{t_1} = \int_{t_0}^{t_1} \frac{w U_c(t)}{\rho c}\, dt \quad (14)$$

$$D_{c,t_1} = D_o + \Delta x_{t_1} \quad (15)$$

$$D_{c,t_1} = D_o \int_{t_0}^{t_1} \frac{w U_c(t)}{\rho c}\, dt \quad (16)$$

The pressure difference between the filter medium and dust cake when $t = t_1$ is

$$\Delta P_{c,t_1} = \frac{k_2 \mu U_c(t_1) D_{c,t_1}}{2} \ln\left[\frac{D_{c,t_1}}{D_0}\right] \quad (17)$$

and

$$U_c(t_1) = \left(\frac{D_0}{D_{c,t_1}}\right) U_o \quad (18)$$

Rearranging equation (17);

$$\Delta P_{c,t_n} = \frac{k_2 \mu U_0 D_0}{2} \ln\left[1 + \frac{\Delta x_{t_1}}{D_0}\right] \quad (19)$$

As the dust accumulates, and the changes of face velocity do not affect the structure of the dust cake, $t = t_n$,:

$$D_{c,t_n} = D_o + \frac{w}{\rho_c}\left[\int_{t_0}^{t_1} U_c(t)\, dt + \int_{t_1}^{t_2} U_c(t)\, dt + \ldots \int_{t_{n-1}}^{t_n} U_c(t)\, dt \right. \quad (20)$$

$$\Delta P_{c,t_n} = \frac{k_2 \mu U_c(t_n) D_{c,t_n}}{2} \ln\left[\frac{D_{c,t_n}}{D_0}\right] \quad (21)$$

Equation (21) can be rewritten as :

$$\Delta P_{c,t_n} = \frac{k_2 \mu U_0 D_0}{2} \ln\left[1 + \frac{\Delta x_{t_n}}{D_0}\right] \quad (22)$$

Total pressure is then rewritten as:

$$\Delta P_{total} = \Delta P_f + \Delta P_{c,t_n} \quad (23)$$

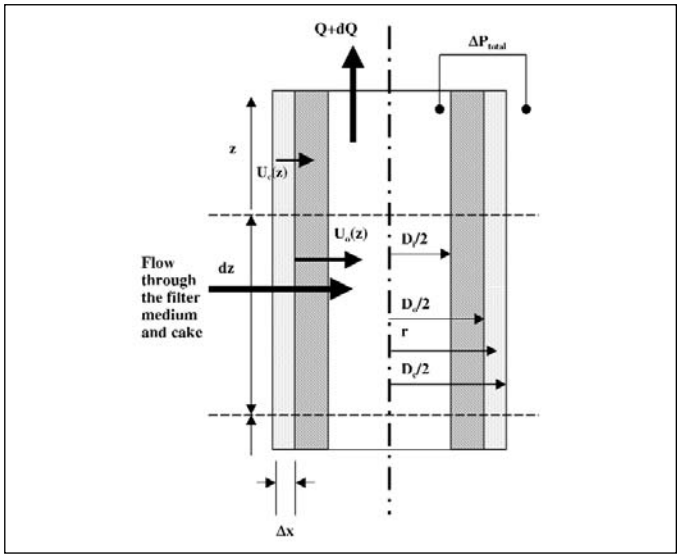

Figure 4: Schematic diagram of flow in a filter section with Filter Cake

And the resistance of flow is

$$R = \frac{(P_o - P)}{\pi D_o U_{o,z}} = \frac{(P_o - P)}{\pi D_c U_{c,z}} \quad (24)$$

where $U_o(z)$ denotes the face velocity (i.e. at the outer diameter of the medium) at position z along the axis (Figure 4). The model now can be written as equation (25) to calculate the pressure difference along the z-axis:

$$\left[\frac{\pi^2 D_i^4}{32\rho}\right] \frac{dP}{dz} = -Q(\pi D_c U_{c,z}) - \frac{fQ^2}{D_i} \quad (25)$$

The cake thickness at position z is;

$$\Delta x = \frac{\Delta z}{L} \int \frac{w U_c(t)}{p_p (1-\varepsilon_c)}\, dt \quad (26)$$

where L is the length of the candle.

Calculation of Cake Resistance

Cake resistance can be calculated by using the Carman-Kozeny equation, together with some assumptions. Assuming that the cake is incompressible and that the particles are spheres that barely touch, then $S_o = 6/d_p$ [5-7]. Taking the porosity of the cake as 0.85, as Schmidt [8] found that the porosity of the dust cake was constant at this value from a distance of 50µm from the surface of the filter medium upwards. The porosity can also be obtained experimentally.

Cake Porosity

The porosity of the filter cake is a very important parameter, as well as the pressure drop in the filter and the necessary force for the removal of the deposited dust layer depend on it. However, due to the high fragility of the dust cake, it is very difficult to measure experimentally. However, Aguiar and Coury [9] presented an experimental technique for measuring the porosity by adapting the work of Schmidt and Löffler [10]. Their comparisons between experimental work and theoretical equations, led them to

conclude that the Ergun correlation can be used for estimating the medium porosity with reasonable accuracy. It is then used here to estimate the cake porosity. For a dust layer of thickness, L, composed of particles with mean diameter, d_p;

$$\frac{\Delta P}{L} = 150\frac{(1-\varepsilon)^2}{\varepsilon^3}\frac{\mu U}{d_p^2} + 1.75\frac{(1-\varepsilon)}{\varepsilon^3}\frac{\rho U^2}{d_p} \quad (27)$$

The mass of particles deposited on the filter is:

$$M = \dot{m}t = LA\rho_p(1-\varepsilon) \quad (28)$$

where $\dot{m}$ is the mass flow rate of particles of density, ρ_p, A is the filtration area and t is the filtration time. Therefore:

$$L = \frac{(Qt)}{[A\rho_p(1-\varepsilon)]} \quad (29)$$

By substituting equation (29) into the Ergun equation (27), it becomes:

$$\frac{\Delta P}{t} = 150\frac{(1-\varepsilon)^2}{\varepsilon^3}\frac{\mu QU}{A\rho_p d_p^2} + 1.75\frac{(1-\varepsilon)}{\varepsilon^3}\frac{\rho QU^2}{A\rho_p d_p} \quad (30)$$

Equation (30) can then be used for estimating the cake porosity from a graph of ΔP vs. t.

Cake Detachment and Pressure Drop Analysis

Several analyses of the problem of cake detachment have been presented, *e.g.* Koch *et al*. [2]. The dust cake is assumed to be detached from the filter medium when it experiences a tensile stress sufficient to overcome either the strength of the adhesive bond between the cake and the medium (or a residual dust layer). In theory, as soon as the strength is exceeded, the cake will be detached simultaneously from the filter surface. However, in practice, the adhesive strength and the applied stress is not entirely uniform across the filter surface resulting in "patchy" cleaning.

In a rigid ceramic filter, the cleaning mechanism is different from that of the fabric filter. There is no displacement on cleaning, therefore, the tensile stress is entirely the result of the pressure drop imposed across the cake due to the reverse flow of cleaning gas. Koch et al. [11] determined the range of tensile stresses over which the cake detaches from the filter medium using a small flat "coupon" of filter medium. Results from the coupon test were plotted in the form of "percentage cake remaining" versus "applied stress", where the applied stress is the appropriate value of the pressure drop across the cake. The curve provided the information needed for selection of a cleaning pressure. Figure 5 shows an example of such curve that might be used in practice. On the left-hand side is a set of cake detachment curves, on the right an imaginary axial distribution of cleaning pressure. If the measured cake detachment stress curve is 'a', then most of the cake will be removed by the pulse; if it is 'c', then very little will. Aguiar and Coury [12], working on detachment of phosphate rock dust from a polyester fabric, showed a good prediction of the cake detachment stress by this approach. The expression σ was then modified by Aguiar and Coury [9] as:

$$\sigma = n_c F_{ad} \quad (31)$$

where F_{ad} is the force of adhesion between two particles and n_c is the average number of particle-particle contacts per unit area:

$$n_c = 1.1(1-\varepsilon)\varepsilon^{-1}d_p^{-2} \quad (32)$$

In the case of dry and inert agglomerates, without the presence of binders or electrostatic charges, the forces of adhesion between the particles are usually due to Van der Waals interactions. For two spheres of the same diameter, d_p, the force can be described as:

$$F_{ad} = \frac{Hd_p}{(24a^2)} \quad (33)$$

where H is the Hamaker constant, which depends on the particle composition (and has a value around 8×10^{-20} J, for most materials of interest [5] and a is the distance of separation

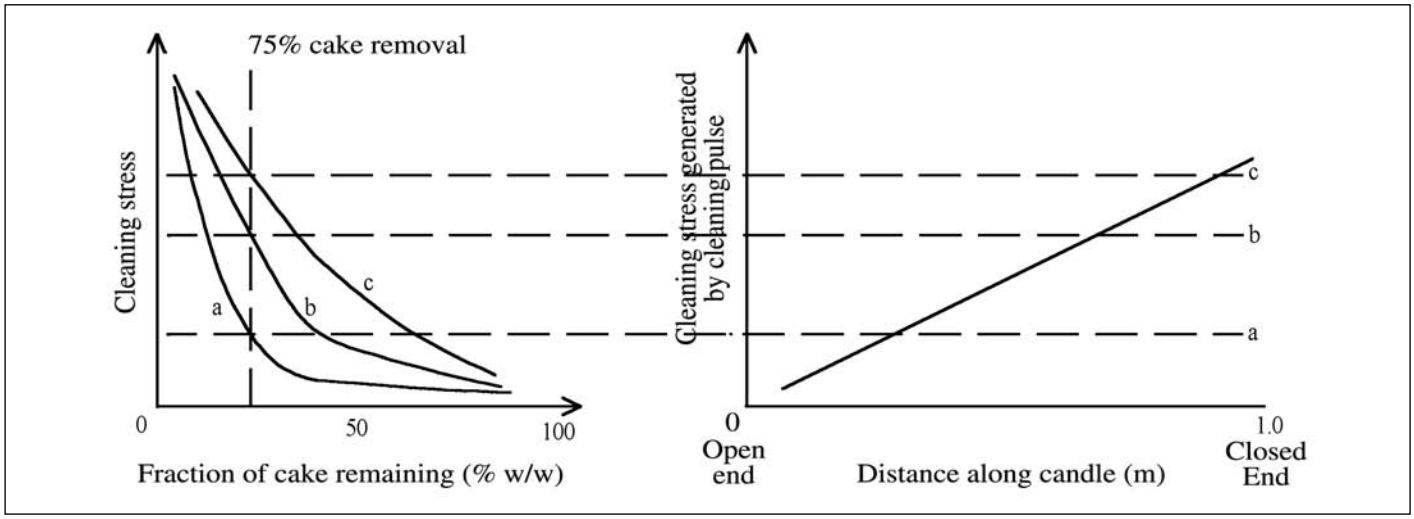

Figure 5: Variation of cake removal with axial position on candle. 'a' indicates the path of cake detachment stress where most of the cake will be removed. If it is on path 'c', very little cake will be removed (Seville, 1999).

Table 1: Parameters used in simulations.

Length of filter, L (m)	1	Resistance to flow, R (Ns/m^4)	22290 (open end) 43120 (closed end)
Inner diameter, D_I (m)	0.042m	Particle density, Limestone, ρ_p (kgm^{-3})	2500
External diameter D_O (m)	0.062	Dust concentration, w (kgm^{-3})	0.01026
Gas viscosity μ (kgm^{-1}s^{-1})	1.7894 x10^{-5}	Cake porosity, ε	0.85
Gas density, ρ_g (kgm^{-3})	1.225	Time interval , Δt (s)	300

between the surfaces of the particles. The cake removal stress can then be written as:

$$\sigma = 0.046 \frac{(1-\varepsilon)\, H}{\varepsilon d_p} \frac{1}{a^2} \tag{34}$$

RESULTS OF SAMPLE CALCULATIONS

A large number of sample calculations were made to ensure that procedures outlined above were valid and workable. The calculation is done by Fortran 90 programming. Some of the results obtained are presented in the following sections. In Table 1, the conditions used for the calculations are outlined. The physical dimensions used here were taken from the previous work of pilot plant study. The carrier gas, air, was taken to be incompressible over the pressure range of interest.

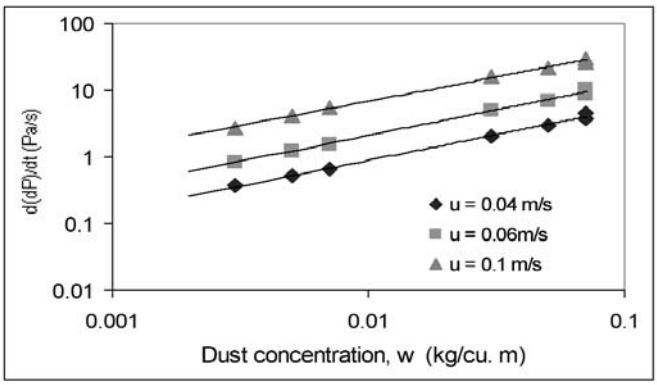

Figure 6: Relationship between the pressure drop increasing rate and the dust concentration under ambient conditions.

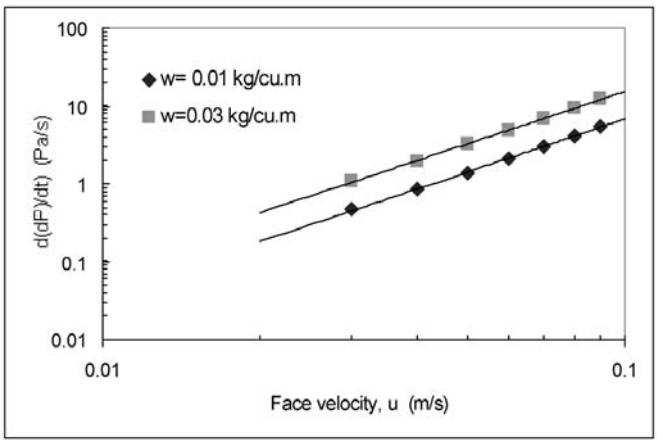

Figure 7: Relationship between the pressure drop increasing rate and the face velocity under ambient conditions.

As discussed previously, the method developed enables one to calculate the total pressure across the filter medium and filter cake. The thickness of the filter cake forming on the surface of the medium for a given face velocity with a constant particle concentration can also be calculated. The concentration w is directly proportional to the total amount of particles to which the filter media are exposed and is the independent variable.

Relationship of Dust Concentration and Face Velocity

The properties of the dust cake formed during filtration depend mainly on the filter face velocity, the filter medium, gas temperature and in particular, the particle properties. An essential feature is the pressure drop in connection with the permeation of the dust cake.

The pressure drop across the cake, ΔP_c depends on the dust concentration and the face velocity. As ΔP_c increases with time, it is more appropriate to use the rate of increase of the pressure drop, $d\Delta P_c/dt$, to express the influence of these factors. By solving those equations described in the section before, which enable the calculation of the pressure drop across the filter cake for the whole filter (*i.e.* for z = 0 to L), the relationships between the rate of increase of the pressure drop and the dust concentration and the face velocity are plotted respectively.

Figure 6, which shows the relationship between the rate of increase of the pressure drop (from the simulation) and the dust concentration under ambient condition, confirming, as expected, that $d\Delta P_c/dt$ is proportional to the dust concentration.

Figure 7 shows the relationship between $d\Delta P_c/dt$ and the face velocity. $d\Delta P_c/dt$ (from the simulation) is proportional to the second power of the face velocity, which follow directly from the Carman-Kozeny equation, which can be rewritten as:

$$\frac{\Delta P}{dL} = \frac{(1-\varepsilon)^2 S_o^2}{\varepsilon^3} \mu u \tag{31}$$

Therefore, for constant dust concentration,

$$\frac{d\Delta P}{dt} = \frac{(1-\varepsilon)^2 S_o^2}{\varepsilon^3} \mu u \tag{32}$$

EFFECT OF THE FACE VELOCITY ON THE CAKE THICKNESS

The cake thickness distribution along the filter surface for different face velocities after an hour of filtration is shown in Figure 7. For those discrete “steps” as seen, corresponding to the five sections of resistance into which the filter was divided for the purpose of the calculation. Each section has a different resistance value. Due to the influence of different local face velocities in the sections along the filter axis this lead to different cake deposition rates at the filter surface.

At higher face velocity, the cake thickness increased dramatically. However, the distribution of the cake thickness was not uniform at any face velocity. The variation in the thickness at different positions on the filter was caused by the non-uniform

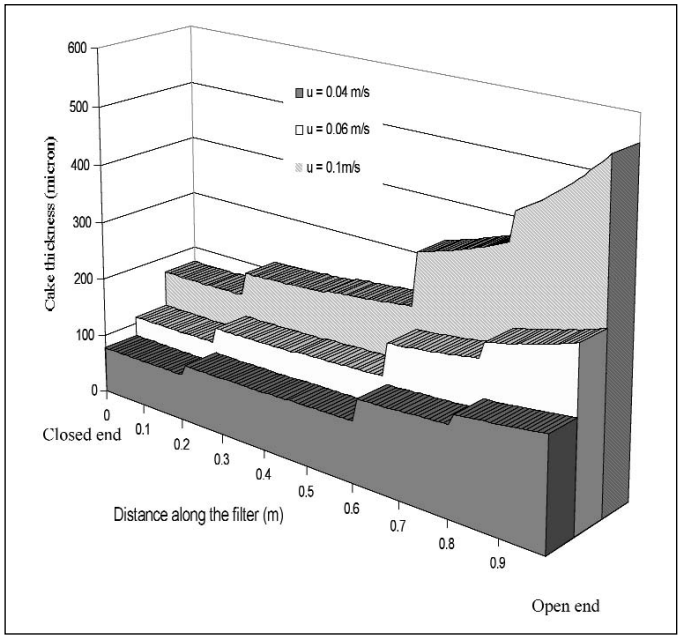

Figure 8: Relationship between the filter cake thickness and the face velocity (t=1 hr) under ambient conditions.

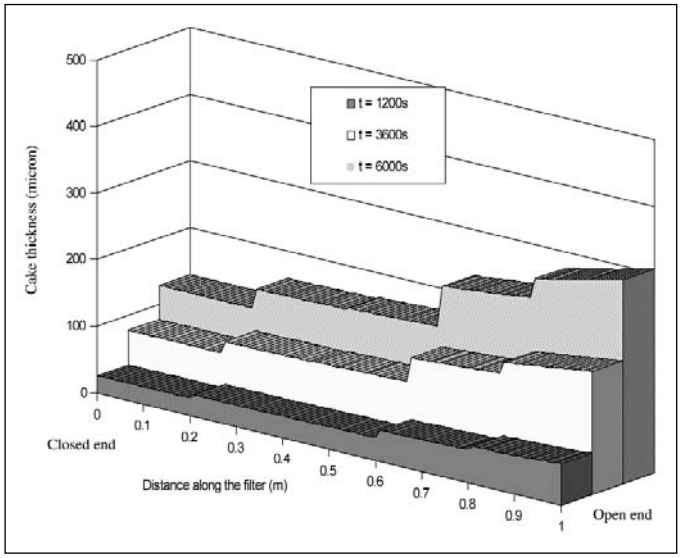

Figure 9: Effect of filtration time on the cake thickness (u = 4 cm/s).

velocity distribution. At a face velocity of 4 cm/s, deposition of dust was more uniform throughout the filter medium than at higher velocities. Dust layers were found to be less than 100µm thick at less than 60cm from the closed end, but much thicker close to the open end. As for the face velocity of 10 cm/s, the dust cake accumulated rapidly at the open end of the filter due to the higher velocity there.

Effect of Filtration Time on the Cake Thickness

The distribution of dust cake thickness with time is shown in Figure 9. As expected, with increasing time the accumulation of dust on the filter surface also increased. Deposition of the dust cake became less uniform on the filter as time increased.

Figure 10 shows the relationship of dimensionless cake thickness, $h/\bar{h}$, along the filter with time ($\bar{h}$ is the average cake thickness). During the early stages of filtration, the cake thickness increment was non-uniform (t = 1200s). But at the longest filtration time, more uniform increments in thickness were seen (t = 3600s). The accumulation of the dust over the filter surface was low at the closed end and was higher close to the open end. Figure 11 illustrates a schematic diagram of cake build up on the surface over time. At the beginning of the filtration (t = 0), no dust cake was formed. When $t = t_1$, the dust deposited on the filter surface and formed a cake layer at the open end of the filter. At $t = t_n$, the

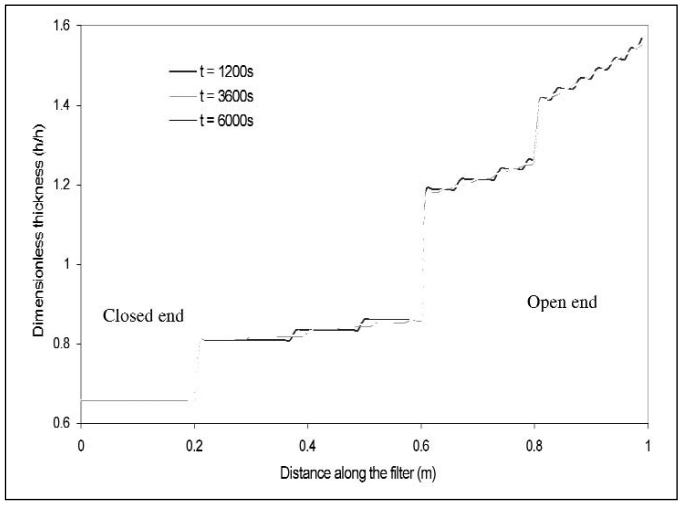

Figure 10: Dimensionless thickness vs. time.

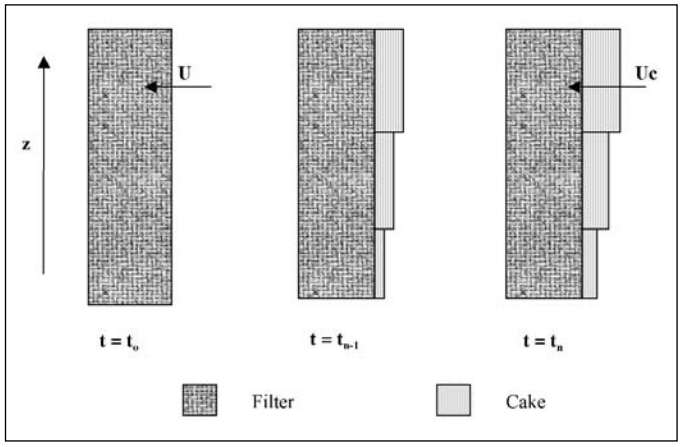

Figure 11: Schematic diagram of cake build-up. The distribution over time is shown by the varied patterns.

dust layer covers the whole surface of the filter and the previous dust layer becomes thicker as more particles deposit on it. In other words, the cake grows from the open end towards the closed end with more particles deposited at the open end due to the higher velocities, hence giving a thicker cake.

Relationship between Cake Velocity Distribution and Cake Thickness

Figure 12 shows the relationship between dust cake deposition and velocity distribution. A non-uniform velocity profile along the filter was observed at t=900s which mirrors the non-uniform local velocity distribution.

Effect of Friction Factors

Figure 13 shows the effect of the friction factor on the total pressure difference. The friction factor makes little contribution to the pressure difference for f =0.05 and 0.1 up to a distance of 60

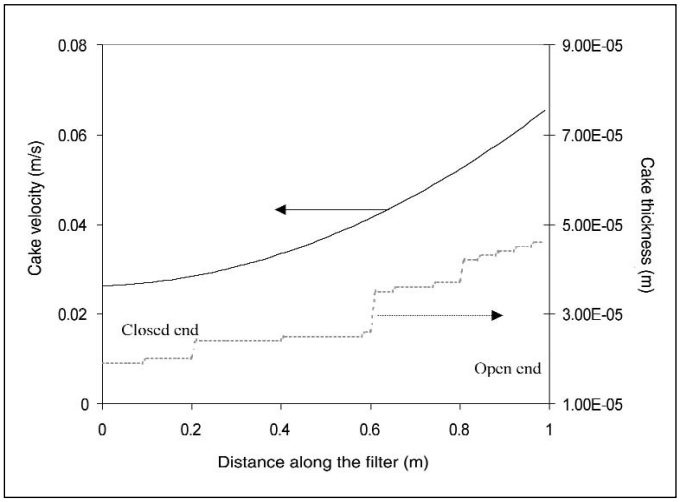

Figure 12: Relationship between the velocity distribution and dust cake thickness at t = 900s (u = 4cm/s).

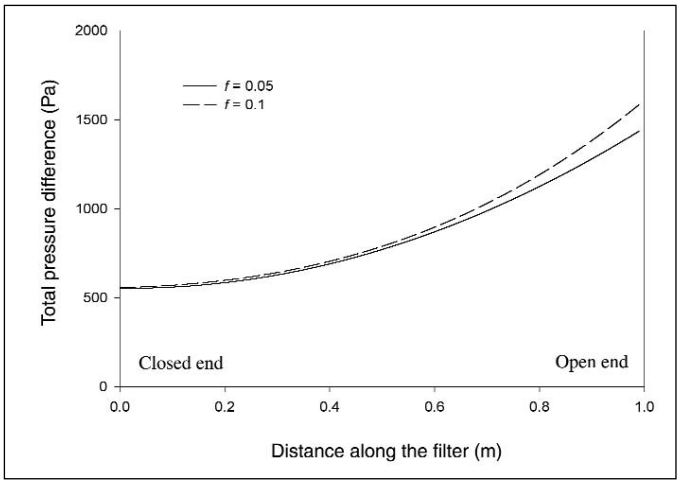

Figure 13: Effect of friction factors on total pressure difference (u=4cm/s).

cm from the closed end. The effect on the pressure difference increased close to the open end, because of the high velocities in this region. (As noted earlier, the frictional pressure drop is roughly proportional to the square of velocity). At this distance the pressure drop caused by friction had been increased. Due to the higher volumetric flowrate with the increasing distance, the momentum of gas flow was also increased. The frictional term will then dominate. At a higher friction factor, the effect on the pressure difference was more significant.

Cake Detachment Simulations

The assumption made in this simulation was that when the pressure difference across the cake exceeds the "detachment stress", detachment of the cake occurred. The detachment stress depends on various factors, including the particle size distribution in the cake, the chemical composition of the particles and temperature. The bonding forces that may occur between the filter medium and the dust cake may increase with time due to the possibility of deformation and sintering of particles [13]. To simplify the model, assumptions of constant cake detachment stress and an incompressible cake were applied.

When the removal stress was applied to the filter, some areas of the filter cake may not be detached as they possess a higher detachment stress. The older cake layers remaining on the surface will then be covered by the new dust layers as time proceeds. Hence, thicker cake layers will be formed. The detachment stress for the dust cake was determined accrording to equation (34). By applying the reverse flow model described by Stephen [14] and Clift *et al*. [15], the applied cleaning stresses on the filter was calculated at various reverse flow volumetric flowrates.

EFFECT OF REVERSE FLOW VOLUMETRIC FLOW RATE

The distribution of dust cake thickness with different reverse volumetric flowrates, are shown in Figure 14 (face velocities 4 cm/s) and Figure 15 (face velocities 6 cm/s). As can be seen in the figures, the dust cake remained in the area near the open end, because the applied stress was lower than the detachment

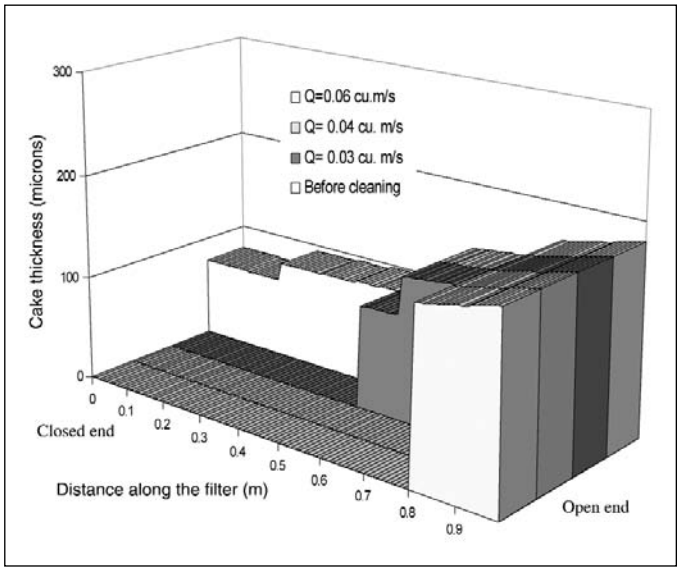

Figure 14: Cake detachment after reverse flow cleaning with a face velocity of 4cm/s.

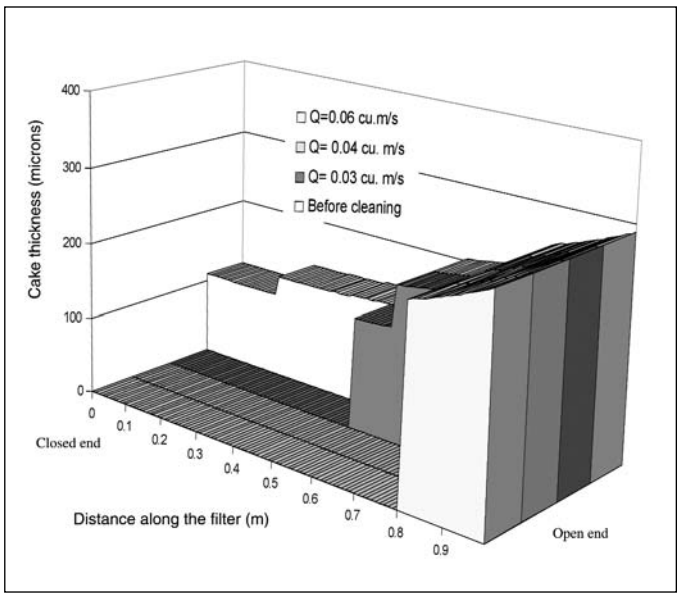

Figure 15: Cake detachment after reverse flow cleaning with a face velocity of 6 cm/s.

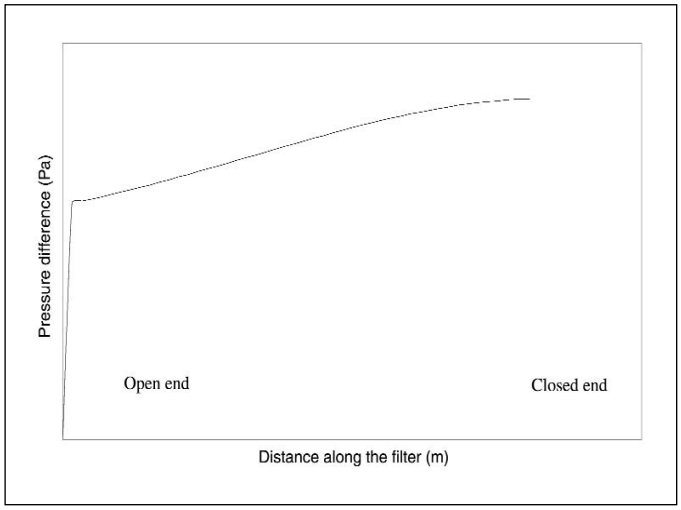

Figure 16: Schematic of diagram of pressure difference distribution of reverse flow cleaning.

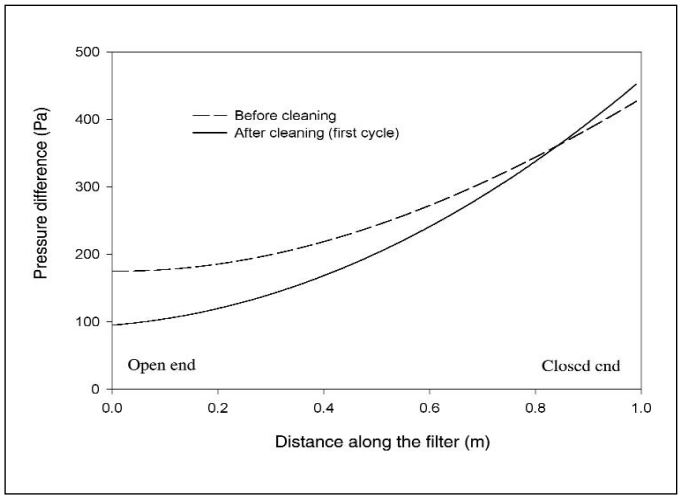

Figure 17: Pressure difference distribution before and after first cycle of cleaning in filtration mode.

stress of the dust cake in that region. Higher volumetric cleaning flow rates will improve the cleaning condition on the filter. However, even at the highest flow rate some fraction of the dust cake still remained on the filter. Detachment of the filter cake occurs more readily at the bottom of the candle because that was where the applied detachment stress was the highest (see Figure 16).

CONDITIONING OF THE FILTER

Figure 17 shows the pressure difference profile before cleaning and after the first cleaning cycle. The pressure drop was reduced in the area where dust cake had been removed. However, close to the open end the pressure drop was increased, due to the fraction of uncleaned dust cake remaining. Now "younger" dust cake will deposited on top of the older filter cake layer, hence increasing the pressure drop.

Using the numerical model, the pressure drop was simulated as a function of time in order to analyse the filter conditioning. Figure 18 shows the simulated pressure difference history for the first five cycles of the filtration with a face velocity of 4 cm/s. The filter was cleaned when the pressure reached 400 Pa. The calculated results show a similar conditioning profile on the rigid

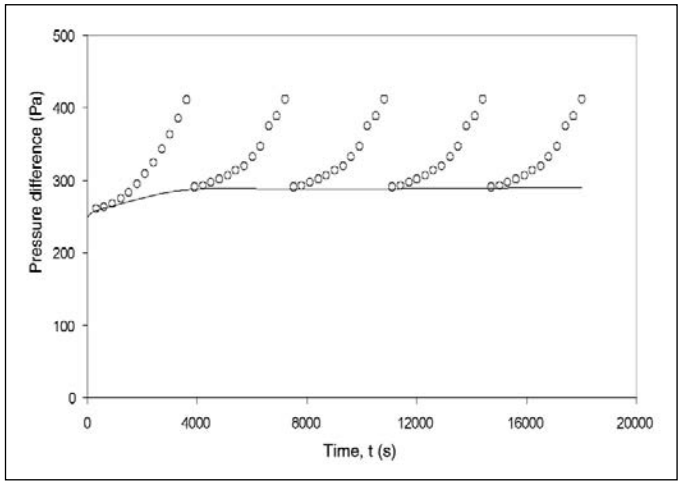

Figure 18: Simulated pressure difference vs. filtration time for a sequence of filtration cycles (4 cm/s).

ceramic filter comparable to the previous findings [16, 17]. The non linear curve indicates that non-homogeneous cake cleaning was occurring throughout the filtration. However, there was not much difference between successive filtration cycles.

CONCLUSIONS

A model has been developed for the combined processes of filtration and cake detachment, incorporating non-uniformity of cake thickness in the axial direction. Results from the cake build-up and detachment model gave an idea of the conditioning process and the development of patchy cleaning on the filter surface.

This model can also be further modified to study the pressure distribution for the compressible dust cake. The detachment stress of the cake depends on various factors, such as particle size distribution in the cake, the chemical composition of the particles, temperature, *etc*. They should also be considered in the improvement of the model. Experiments should also be carried out in order to improve the model under more realistic operation parameters.

REFERENCES

[1] J. P. K. Seville, W. Cheung and R. Clift, A Patchy-Cleaning Interpretation of Dust Cake Release From Non-Woven Fabric, *Filtration and Separation,* 26(2), 187-190 (1989).

[2] D. Koch, J. P. K. Seville and R. Clift, Dust Cake Detachment from Gas Filters, *Power Technology,* 86, 21-29 (1996).

[3] C. Tien, R. Bai and B. V. Ramarao, Analysis of Cake Growth in Cake Filtration: Effect of Fine Particle Retention, *AIChE J.,* 43(1), 33-44 (1997).

[4] J. P. K. Seville, R. Clift, C. J. Withers and W. Keidel, Rigid Ceramic Media for Filtering Hot Gases, *Filtration and Separation,* 26(3), 265-271 (1989).

[5] J. P. K. Seville, U. Tuzun and R. Clift, *Processing Solid Particulate Solids,* pp. 261-297 Blackie Academic and Professional, Glasgow (1996).

[6] H. E. Hesketh, *Fine Particles in Gaseous Media,* pp. 109-113, Lewis Publishers, Inc.,Michigan (1986).

[7] K. Ushiki and C. Tien , Analysis of Filter Candle Performance, *Powder Technology,* 58, 243-258 (1989).

[8] E. Schmidt, Simulation of Three Dimensional Dust Cake Structures via Particle Trajectory Calculations for Cake-Forming Filtration, *Powder Technology,* 86, 113-117 (1996).

[9] M. L. Aguiar and J. R. Coury, Cake Formation in Fabric Filtration of Gases, *Ind. Eng. Chem. Res.,* 35, 3673-3679 (1996).

[10] E. Schmidt and F. Löffler, Preparation of Dust Cakes for Microscopic Examination. *Powder Technology,* 60, 173-177 (1990).

[11] D. Koch, K. Schulz, J. P. K. Seville and R. Clift, Regeneration of Rigid Ceramic Filters, in: *Gas Cleaning at High Temperatures,* R. Clift and J. P. K. Seville (Eds), pp. 244-265, Blackie Academic & Professional, London (1993).

[12] M. L. Aguiar and J. R. Coury, Air Filtration in Fabric Filters: Cake-Cloth Adhesion Force, *Journal of Fluid/ Particle Separation,* 5, 193-198 (1992).

[13] W. Duo, J. P. K. Seville, N. F. Kirkby, H. Büchele, and C. K. Cheung, Patchy Cleaning of Rigid Ceramic Filters. Part 1: A Probabilistic Model, *Chemical Engineering Science,* 52(1), 141-151 (1997).

[14] C. M. Stephen, Filtration and Cleaning Behaviour of Rigid Ceramic Filters, PhD Thesis, University of Surrey (1997).

[15] R. Clift, J. P. K. Seville and J. W. W. ter Kuile, Aerodynamic Considerations in Design and Cleaning of Rigid Ceramic Filters for Hot Gases in: *Proc. of 5th World Filtration Congress,* pp. 530-537. Nice (1990).

[16] Duo, W., Kirkby, N. F., Seville, J. P .K., Clift, R. (1997b). "Patchy Cleaning of Rigid Ceramic Filters. Part 2: Experiments and Validation". Chemical Engineering Science, 52(1), pp. 153-164.

[17] Grannell, S. K. (1998). "The Industry Application of Low Density Rigid Ceramic Filters for Hot Gas Cleaning". PhD Thesis, University of Birmingham.

NOMENCLATURES

a	distance of separation between the surfaces of the particles	m
D_i	filter inner diameter	m
D_o	filter outside diameter	m
d_p	particle diameter	m
F	total shear force	N
F_{ad}	adhesion force	N
f	Fanning friction factor	-
H	Hamaker constant	J
h	Cake thickness	m
k_1	first Ergun equation constants	$kg^{-1}m^{-1}$
k_2	second Ergun equation constant	m^{-1}
L	length of the filter section	m
M	total massretained in the filter system.	kg
$\dot{m}$	mass flowrate	kg/s
n_c	average number of particle-particle contacts per unit area	m^{-2}
P	pressure	N m^{-2}
D_{Pf}	pressure dropover filter medium	N m^{-2}
D_{Pc}	pressure drop over cake	N m^{-2}
DP_T	pressure drop over cake plus medium	N m^{-2}
Q	actual volumetric flow rate	m^3 s^{-1}
R	specific resistance	m^{-1}
r	radius	m
S_o	specific surface area	m^{-1}
Δt	time interval between (t-1) and t	-
U	superficial gas velocity	m s^{-1}
u	gas velocity	m s^{-1}
w	areal cake loading	kg m^{-2}
Δx	cake thickness	m
Δz	incremental distance	m

GREEK

ε	porosity	-
εc	cake porosity	-
μ	fluid viscosity	$kgm^{-1}s^{-1}$
ρ	fluid density	kg m^{-3}
ρ_c	cake density	kg m^{-3}
ρ_g	gas density	kg m^{-3}
ρ_p	solid (particle) density	kg m^{-3}
σ	cake removal stress	N m^{-2}